

Chapter 7

Advantages of Radiochemistry in Microliter Volumes

Pei Yui Keng, Maxim Sergeev, and R. Michael van Dam

Abstract Positron emission tomography (PET) provides quantitative 3D visualization of physiological parameters (e.g., metabolic rate, receptor density, gene expression, blood flow) in real time in the living body. By enabling measurement of differences in such characteristics between normal and diseased tissues, PET serves as vital tool for basic research as well as for clinical diagnosis and patient management. Prior to a PET scan, the patient is injected with a short-lived tracer labeled with a positron-emitting isotope. Safe preparation of the tracer is an expensive process, requiring specially trained personnel and high-cost equipment operated within hot cells. The current centralized manufacturing strategy, in which large batches are prepared and divided among many patients, enables the most commonly used tracer (i.e., [^{18}F]FDG) to be obtained at an affordable price. However, as the diversity of tracers increases, other strategies for cost reduction will become necessary. This challenge is being addressed by the development of miniaturized radiochemistry instrumentation based on microfluidics. These compact systems have the potential to significantly reduce equipment cost and shielding while increasing diversity of tracers produced in a given facility. The most common approach uses “flow-through” microreactors, which leverage the ability to precisely control reaction conditions to improve synthesis times and yields. Several groups have also developed “batch” microreactors which offer significant additional advantages such as reduced reagent consumption, simpler purifications, and exceptionally high specific activity, by reducing operating volumes by orders of magnitude. In this chapter, we review these “batch” approaches and the advantages of using small volumes, with special emphasis on digital microfluidics, in which reactions have been performed with volumes as low as $\sim 1 \mu\text{L}$.

Keywords Microfluidics • Radiosynthesis • Positron emission tomography (PET) • Electrowetting-on-dielectric (EWOD) • Microscale chemistry

P.Y. Keng • M. Sergeev • R.M. van Dam (✉)
Crump Institute for Molecular Imaging and Department of Molecular and Medical
Pharmacology, David Geffen School of Medicine, University of California, Los Angeles, CA,
USA
e-mail: mvandam@mednet.ucla.edu

7.1 Introduction

7.1.1 *Radiosynthesis of Positron Emission Tomography Tracers*

Positron emission tomography (PET) is an extremely powerful, noninvasive diagnostic imaging technology capable of measuring a plethora of biological processes in vivo [1]. In research, PET can provide dynamic information about normal or diseased states of a living organism and, in the clinic, can provide information that is critical for diagnosis, selection of therapy, or monitoring response to therapy. In some cases, PET can detect biochemical changes associated with disease before any anatomical changes can be observed [2].

PET requires injection of a tracer labeled with a positron-emitting isotope, such as fluorine-18, nitrogen-13, oxygen-15, carbon-11, or a radiometal. Fluorine-18 possesses physical and nuclear properties that are particularly desirable for radiolabeling and imaging [3]. For example, the low positron energy and range ensure high-resolution imaging while minimizing radiation exposure to the patient. In addition, the 110 min half-life is sufficiently long for multistep synthesis, transport to the imaging site, and imaging over extended periods.

Due to the hazard of working with radioactive materials, a specialized infrastructure of automated radiosynthesizers operating in radiation-shielded “hot cells” by expert personnel is required. Due to the high costs, a couple of tracers (including 2- ^{18}F fluoro-2-deoxy-D-glucose, ^{18}F FDG) are currently produced in a “satellite” manner. Radiopharmacies manufacture large batches that are subdivided among many patients within a local area to leverage economies of scale and offer the compound at an affordable price. As the diversity of PET tracers used in medical care and research increases, opportunities to share costs are reduced, and alternative innovative approaches are needed to reduce the high cost of each batch.

A particularly promising approach is the development of miniaturized radiosynthesizers based on microfluidic technology that can enable dramatic reductions in the cost of equipment and the amount of radiation shielding needed. An additional innovation is the concept of disposable “cassettes,” which allows each synthesizer to make a wide range of tracers simply by using different cassettes, rather than being dedicated to production of a single tracer [4].

7.1.2 *Microfluidics for Radiosynthesis*

It has been well established that the geometry of microfluidic devices offers many advantages for the synthesis of short-lived radiopharmaceuticals [5–7]. In particular, the small dimensions enable improved control of reaction conditions via rapid mixing and efficient heat transfer, leading to faster reactions and improved selectivity, thus higher yields.

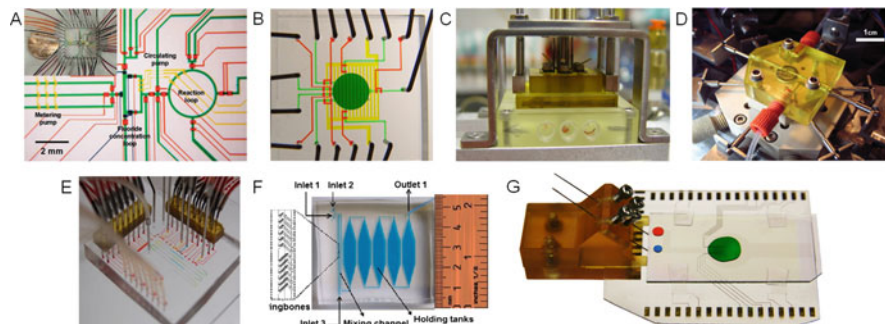


Fig. 7.1 Batch microfluidics devices for synthesis of PET tracers: (a) PDMS chip with 40 nL reactor (Adapted from reference [14] with permission from AAAS). (b) Scaled-up PDMS chip with 5 μ L reactor (Adapted from reference [15], Copyright © 2010 by the Society of Nuclear Medicine and Molecular Imaging, Inc.). (c) Chemically inert polydicyclopentadiene (pDPCPD) polymer chip with 5 μ L reactor (Reproduced from reference [56]). (d) Chemically inert pDPCPD chip with 60 μ L reactor (Reproduced with permission from reference [50], Copyright © 2010 John Wiley & Sons, Ltd.). (e) PDMS chip for optimizing radiolabeling reaction in variable volume droplets (~100 nL) (Reproduced with permission from reference [59], Copyright © 2015 IOP Publishing). (f) PDMS chip for radiometal labeling with 25 μ L reaction volume (Reproduced with permission from reference [19], Copyright © 2013 Elsevier, Inc.) (g) EWOD chip with reaction volume ranging from 2 to 17 μ L

Most commonly in the field of radiochemistry, these devices are based on “flow-through” microreactors, where reactions occur by flowing reagent streams through mixers and preheated capillary tubes or microchannels. Numerous groups have demonstrated the radiosynthesis of [18 F]FDG in polymer chips [8], glass chips [9], and capillary tubes [10]. This technology has been commercialized (e.g., Advion Biosciences “NanoTek” and Scintomics “ μ -ICR”), and dozens of different radiotracers labeled with F-18, C-11, N-13, and Tc-99 m have been demonstrated [11]. Recent advances have enabled the integration of solvent exchange processes [12, 13], which previously were accomplished via bulky, off-chip subsystems.

Because it is important that flow-through systems are completely filled with liquid in order to achieve accurate fluid handling, typical operating volumes are comparable to macroscale systems (i.e., >500 μ L). Another class of microfluidic device based on small (<50 μ L) volumes known as “batch” microreactors have also been used for radiochemistry (Fig. 7.1). These devices are particularly attractive for radiochemistry because all synthetic steps including solvent exchange can be integrated into a single chip and because small volumes can reduce reagent consumption, enhance reaction kinetics, improve specific activity, reduce radiolysis, and simplify purification, as described below.

7.1.3 Platforms for Microliter Volume Synthesis

The first batch microfluidic synthesis of [18 F]FDG was demonstrated in a polydimethylsiloxane (PDMS) chip with 40 nL reaction volume [14]. Microvalves

were used to close the reactor during reaction steps, and the permeability of the PDMS enabled escape of vapor for solvent exchange processes. By scaling up the reactor volume to 5 μL , it was possible to produce mCi amounts of [^{18}F]-labeled tracers [15]. Unfortunately, due to adverse interaction of PDMS with [^{18}F]fluoride [16], radioactivity losses were high and reliability was low. Using inert plastic materials as the reaction vessel improved reliability, and a system with 50 μL reaction volume enabled production of tracers of sufficient quantity and quality for human imaging [17], establishing the relevance of the micro-batch format.

While the PDMS chip was not suitable for processing [^{18}F]fluoride, the capability to react small volumes was found to be useful for screening radiolabeling conditions for the reaction of [^{18}F]SFB with an engineered antibody [18]. Using <100 nL per droplet, many reaction conditions could be tested, and then the whole batch could be labeled once optimal conditions were found. A quasi-continuous-flow PDMS chip using small volumes (25 μL) has also been used for radiolabeling peptides and proteins with radiometals such as Ga-68 and Cu-64 [19]. The small volume enabled improved stoichiometry of the label and ligand, dramatically improving the labeling yield and potentially avoiding the need for extensive purification.

Recently, our group demonstrated successful radiosynthesis of [^{18}F]FDG and other molecules using another type of batch microfluidic device based on the digital manipulation of droplets between two parallel plates [20, 21] known as electrowetting-on-dielectric (EWOD). Droplets are controlled by on-chip electrodes (Fig. 7.2), eliminating the need for bulky valve actuators, pumps, and radiation shielding as is needed in the approaches mentioned above. A wide range of reagents and reaction conditions can be used on these EWOD microchips because they are constructed from inert and thermally stable materials (glass substrate, metallic electrode layer, inorganic dielectric layer, and fluoropolymer layer). Because droplets are surrounded by gas, evaporation and solvent exchange can readily be performed on the chip. Resistive heating, temperature sensing for precise temperature control, and impedance sensing for measuring electrical properties of liquid can all be integrated on the chip without the need of additional bulky hardware [22].

Using this platform, our laboratory has reported the successful synthesis of [^{18}F]FDG [20], 3-[^{18}F]fluoro-3'-deoxy-fluorothymidine ([^{18}F]FLT) [23], [^{18}F]fallypride [24], and N-succinimidyl 4-[^{18}F]fluorobenzoate ([^{18}F]SFB) [25] with radiochemical yields of $22 \pm 8\%$ ($n = 11$), $63 \pm 5\%$ ($n = 5$), $65 \pm 6\%$ ($n = 7$), and $19 \pm 8\%$ ($n = 5$), respectively. The final ^{18}F -labeled compounds passed all quality control tests required by the United States Pharmacopeia for injection into humans and have been successfully used in preclinical PET. The syntheses of [^{18}F]FDG and [^{18}F]FLT on a simplified EWOD chip have also been reported by others [26, 27]. These results suggest that the EWOD-based synthesizer can meet the requirements for on-demand production of diverse PET tracers to meet preclinical or clinical needs.

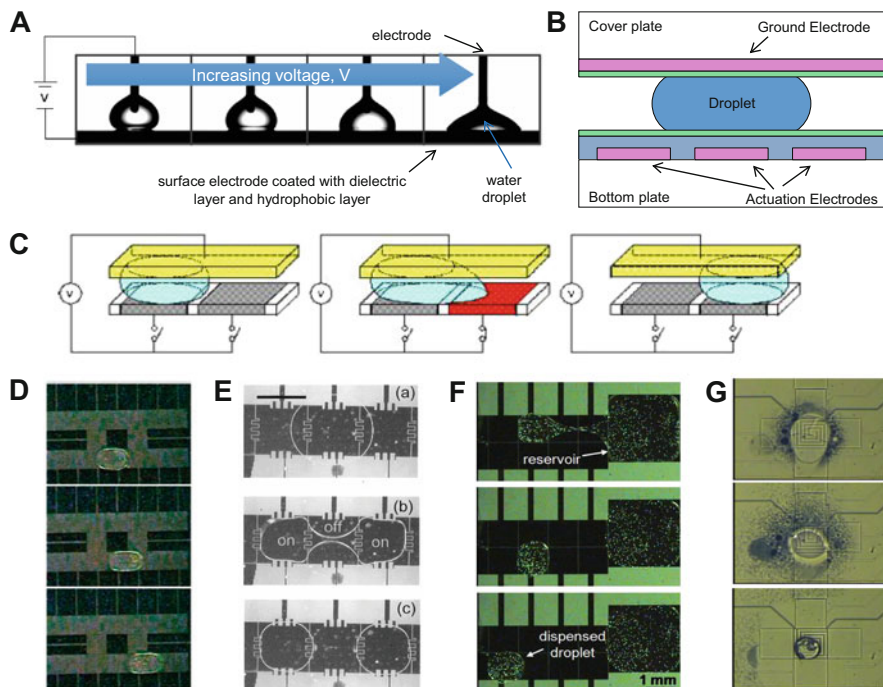


Fig. 7.2 Structure and operation of EWOD microfluidic chips. (a) Illustration of the “electrowetting” effect. (b) Schematic of typical EWOD device with droplet sandwiched between the two plates. (c) Applying a local field to one end of the droplet using a small control electrode (typically 1 or 2 mm square) can generate a force on the droplet in a direction toward the activated electrode (Diagram courtesy of Robin Garrell). This force enables several operations, including (d) droplet transport along a predetermined path, (e) droplet splitting, and (f) droplet dispensing from an on-chip reservoir. Incorporation of specialized heating electrodes permits additional operations such as (g) evaporation of solvent. ((d) is reproduced with permission from reference [60] (Copyright © 2004 American Chemical Society), (e) is reproduced with permission from reference [61] (Copyright © 2003 IEEE), (f) is reproduced from reference [62] with permission of The Royal Society of Chemistry.)

7.2 Advantages of Radiosynthesis at the Microliter Scale

7.2.1 Miniaturization and Disposability

Perhaps the most significant potential advantage of batch microfluidics in the field of radiochemistry is the potential to integrate the entire synthesis, purification, and formulation apparatus into an extremely compact system. Size of the components that need to be shielded (because they contain or contact radioactivity) has a tremendous impact on the amount of radiation shielding needed. For a constant thickness “shell” of shielding, t , the volume (and weight and cost) of the shielding scale is

$$\begin{aligned}\text{Shielding volume} &\sim (r+t)^3 - r^3 = (3r^2t + 3rt^2 + t^3) \\ &= 3r^2t \left(1 + \frac{t}{r} + \frac{1}{3} \frac{t^2}{r^2} \right)\end{aligned}$$

where r is the dimension of the synthesizer. Assuming a fixed shielding thickness where $t \ll r$, the scale factor is proportional to r^2 . Thus, moving from macroscale systems with ~20-inch dimensions to microfluidic chips with ~2-inch dimensions can reduce the needed shielding 100-fold. This reduction could make it practical for radiochemistry chips to be used in benchtop situations instead of needing to operate them in specialized facilities equipped with hot cells and mini cells to shield radiation, thus removing one of the bottlenecks in PET tracer production.

Integrating the fluid pathways of a radiosynthesizer into a microfluidic chip has other advantages as well. If the chip can be made to be very inexpensive, the entire fluid pathway can be discarded after each synthesis run, eliminating the need for developing and validating a cleaning protocol and associated documentation or cleaning the system on a daily basis. This concept of disposability is increasingly being used in macroscale synthesizers to simplify setup, cleanup, and compliance with cGMP manufacturing guidelines for PET tracers that are used in humans [4]. Disposable cassettes also provide flexibility: with a single synthesizer instrument, the operator can choose to install different disposable cassettes (with different pre-configured fluid path configurations) along with matching reagent kits to make different PET tracers [4].

7.2.2 Reduced Radiolysis

Radiolysis is the process of chemical bond cleavage caused by radiation. Molecules of a PET probe undergo irradiation from both the starting [^{18}F]fluoride (external radiolysis) and from other radiolabeled molecules (autoradiolysis) [28–30], which can lead to reduction in the yield of the probe and the formation of radioactive side products. The mechanism of damage is believed to be related to the formation of radical species in the solvent by high-energy particles [29]. While the final injectable formulation can be stabilized against autoradiolysis with addition of radical scavengers (*e.g.*, ethanol) to preserve radiochemical purity [30], this is not generally possible at earlier stages during the radiosynthesis process.

Fluorine-18 emits positrons with high energy ($E_{\text{max}} = 0.633$ MeV) that cause ionization of the solvent while dissipating their kinetic energy along their travel range. The range is up to ~2.4 mm, but due to the tortuous path they follow, the distribution of final displacements of positrons from their origin is characterized by a smaller range (*i.e.*, full width at one third maximum ~1 mm) [31]. When the reaction vessel dimensions (*e.g.*, vial, flask, or Eppendorf tube: ~10 mm) are much greater than this range, each positron deposits all of its energy into the solvent, leading to extensive radiolysis (Fig. 7.3a).

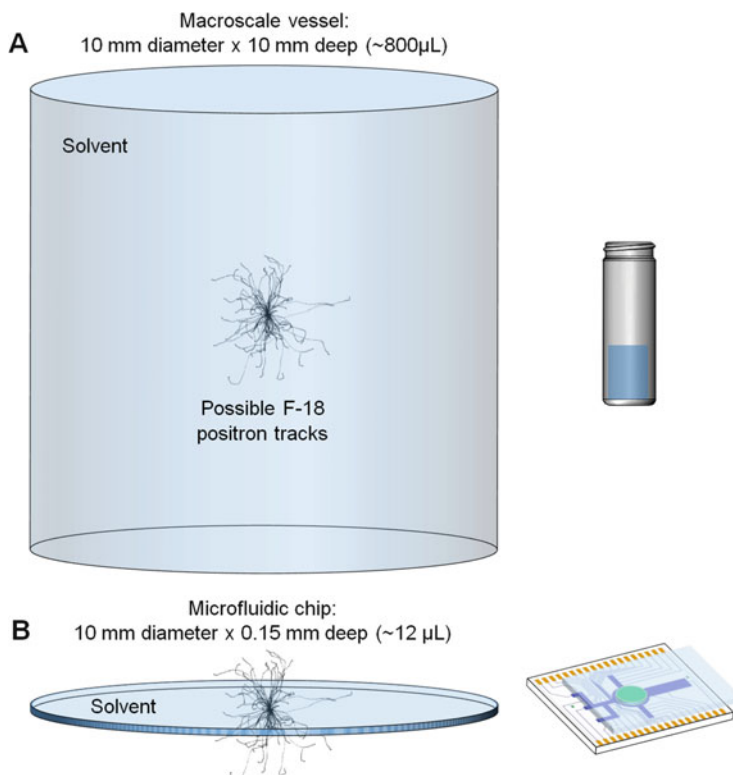


Fig. 7.3 Illustration of radiolysis suppression. (a) Possible positron tracks from decay of a fluorine-18 atom at the center of a conventional macroscale reaction vessel. Because the positron range is significantly less than the reactor dimensions, the positron will deposit all of its energy into the solvent, where it causes radiolysis. This is true of decay events happening throughout the vial. (b) In contrast, in an EWOD microfluidic chip, one dimension of the solvent volume is very thin compared to the positron range. Thus, a significant portion of the possible tracks are mostly or entirely outside the droplet. Thus, most positrons will escape the solvent after having only deposited a small fraction of their energy in the solvent, reducing radiolysis

Rensch et al. have shown via simulations and experiments that the degree of radiolysis is geometry dependent [3]. In vessels for which at least one dimension is significantly smaller than the positron range (e.g., capillary tubing or EWOD chips), there is significantly reduced radiolysis because positrons can escape the solvent before depositing very much of their energy (Fig. 7.3b). For example, the solvent within a 100 μm diameter capillary reactor absorbs only 10 % of the energy

of positrons emitted from within the solvent, and a planar droplet geometry with 100 μm height (similar to the EWOD chip) absorbs only 40 % of the positron energy [32]. Further reduction could be achieved by reducing the dimensions.

7.2.3 *Reagent Minimization*

Because batch microfluidic chips such as EWOD handle volumes that are 2–3 orders of magnitude less than conventional systems, the quantity of reagents needed to perform reactions is proportionately reduced, thereby reducing the per-run reagent cost. Generally the precursor is the most expensive reagent. In macroscale synthesis, reagents for common small-molecule PET tracers can cost hundreds of US\$ for a single synthesis run (e.g., 10 mg in ~ 1 mL). Synthesis in microliter volumes (e.g., 10–100 μg precursor) could reduce this cost down to dollars per run (depending on costs of packing this small amount of reagent into vials), making it economical to produce even small batches on demand for a single user. Biomolecule-based precursors such as proteins are even more expensive, costing up to thousands of US\$ for a single synthesis. Using microliter volumes, the 100 s of micrograms quantity typically used for protein labeling could be reduced to microgram or submicrogram levels. Reducing the reagent consumption enables a greater number of runs per a given amount of precursor or reduces the cost per run of precursor.

Minimization of reagents can also simplify purification processes [19]. Typically in ^{18}F -radiochemistry, the amount of precursor is many orders of magnitude higher than the amount of ^{18}F fluoride to ensure the fluorination reaction occurs as rapidly as possible. For example, in the synthesis of ^{18}F FDG, one typically uses about 40 μmol of mannose triflate [33], compared to the 600 pmol of ^{18}F fluoride ion in a 1000 mCi batch, representing an excess of 5 orders of magnitude. Even accounting for typical final specific activity, the amount of ^{19}F fluoride + ^{18}F fluoride is about 60–600 nmol, meaning there is still an excess of about 2–3 orders of magnitude of precursor compared to (^{18}F + ^{19}F)FDG. This means that at the end of the synthesis, there are vast amounts of unreacted (or hydrolyzed) precursor that must be separated from a much smaller amount of the desired product. Because of the high amounts of precursor, large reaction volume, and the chemical similarity between precursor (native or hydrolyzed) and product, long semi-preparative HPLC purification times may be needed, resulting in a large solvent volume in the purified product. While suitable for patient use, these large volumes can be problematic for imaging in small animals, where the tracer must be sufficiently concentrated to inject enough radioactivity for imaging (typically 100–200 μCi) within the maximum recommended injection volume to avoid physiological perturbation (e.g., <100 μL for mice). Using smaller amounts of reagents in microfluidic formats, several groups have demonstrated that analytical-scale HPLC is sufficient for purification [24, 34], resulting in more concentrated final

formulation. Purification has also been successfully performed with on-chip structures similar to typical macroscale Sep-Pak cartridges [35–37].

Reduced amount of reagents may also simplify the quality control (QC) testing that is needed prior to injection in humans. In general, the reduced amounts of reagents and solvents will lead to reduced amounts of residual impurities after the purification process. An interesting prospect of using extremely tiny volumes is that if the total amount of reagent added is below the injectable limits set by various regulatory agencies, then a test for the absence of that particular chemical may become unnecessary.

7.2.4 High Specific Activity

The specific activity (SA) of a PET tracer (e.g., labeled with fluorine-18) is defined as the ratio of the number of ^{18}F -labeled molecules to the total number of ^{18}F -labeled and ^{19}F -labeled molecules and is typically reported in units of radioactivity per mass (e.g., $\text{Ci}/\mu\text{mol}$). For a certain desired injected dose (e.g., 10 mCi for humans), the higher the SA, the lower the mass that is injected.

High SA of a PET tracer is important for several reasons. First, because many PET tracers are based on pharmacologically active compounds, only a very low mass should be injected to avoid eliciting a pharmacological response. Second, for tracers that target low-abundance receptors (e.g., in neurological imaging), injecting lower mass avoids saturation or high occupancy of the receptors. This is especially important in small animal imaging, in which significantly higher radioactivity is injected (per mass of the animal) compared to human subjects to achieve sufficient image quality with the higher resolution (smaller voxel size) scanners that are used for animals [38]. Third, high SA may improve image quality by increasing the proportion of targets occupied by radioactive forms of the tracer while reducing competitive interactions of the nonradioactive forms. Other reasons to maximize SA are related to the logistics of PET tracer production. Often, tracers need to be transported from the radiopharmacy where they are produced to the imaging center. Because of the radioactive decay during this transport time, the SA is reduced by a factor of 2 for each half-life, and a high initial SA is needed to ensure sufficient SA at the time of imaging.

For fluorine-18, the maximum theoretical SA is $1710 \text{ Ci}/\mu\text{mol}$; however, the actual SA of the final tracer is significantly lower, typically $1\text{--}10 \text{ Ci}/\mu\text{mol}$ [39]. This means the number of fluorine-18 atoms is dwarfed ($\sim 200\text{--}2000\text{X}$) by the number of fluorine-19 contaminant atoms. Some of the fluorine-19 contamination originates due to the equipment and materials used in the $[^{18}\text{F}]$ fluoride production process (e.g., $[^{18}\text{O}]\text{H}_2\text{O}$ quality, volume of target, target materials, tubing materials, target loading/unloading process, etc.) [40–42]. While such sources may be out of most radiochemists' control, another significant contribution is the contamination of reaction mixture with extra fluorine-19 fluoride during the synthesis process itself (i.e., all steps upstream of and including the fluorination step). The main sources are the QMA cartridges used in the fluoride drying process, fluorinated materials (e.g.,

Teflon tubing and stirbars) [43], and the reagents used in the synthesis, such as K_2CO_3 , Kryptofix, etc.

In preliminary studies, our group observed that microfluidic synthesis on EWOD chips resulted in significantly higher (up to 25–50 times) SA compared to macroscale synthesis, starting with the same amount of radioactivity [23, 24]. This suggested the potential for microfluidics to significantly reduce fluorine-19 contamination in the synthesis process. An in-depth investigation led to the observation that the dependence of SA on reaction parameters was very different for macroscale (100–5000 μL) and microscale (2–8 μL) syntheses. At the macroscale, the SA strongly varied with the reaction volume (amount of reagents) as well as the starting radioactivity (from 10s to 100 s of mCi), whereas the SA was much higher and nearly constant (20–23 Ci/ μmol), under all conditions when performed in microdroplets. These results suggest that in the macroscale synthesis, reagents and solvents are the dominant source of fluorine-19, while in microscale volumes, these sources have been nearly eliminated and the fluorine-19 contribution from the cyclotron dominates [44, 45] (Fig. 7.4). The effect of the 120 nm Teflon layer on the chip was also investigated and no impact on SA was seen [43], perhaps due to the radiolysis suppression effect described above.

Small volumes are extremely beneficial for another type of reaction, namely, isotopic exchange (IEX). In IEX reactions, the precursor is identical to the final product, except for the presence of fluorine-19 instead of fluorine-18, and cannot be separated after synthesis. Thus it is desirable to minimize the amount of excess precursor to maintain high SA. In macroscale reactions this is difficult, because the

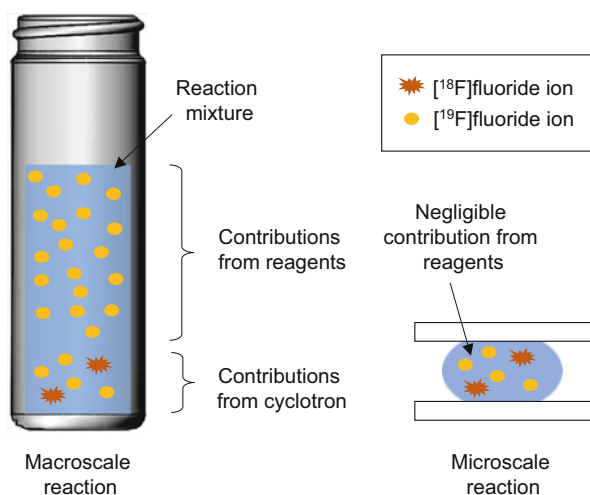


Fig. 7.4 Illustration of specific activity improvement. (Left) At the macroscale, reagents are the dominant source of fluorine-19 contamination in the fluorination reaction mixture. (Right) At the microscale, the reagents add negligible fluorine-19 contamination to that already present from the cyclotron. After the fluorination reaction, the fluoride (both F-18 and F-19 forms) get incorporated into the precursor and cannot be separated, resulting in ^{18}F - and ^{19}F -labeled forms of the tracer

concentration of precursor needs to be sufficiently high for efficient reaction. However, Perrin et al. have shown that small volume reactions are an effective way to minimize precursor amount for IEX reactions [46, 47]. It should be noted that the same principles can be applied to other carrier-added situations or to the labeling of proteins or other species where the labeled and unlabeled forms cannot be separated; in all such cases, it is critical to minimize the starting material in order to obtain high SA. The dependence of SA on starting radioactivity for IEX reactions was investigated in simplified EWOD chips using rhodamine clicked to an aryl-BF₃ moiety [44]. Unlike in nucleophilic substitution reactions, SA of microfluidic IEX reactions was found to vary with starting radioactivity, but in a nonlinear manner. This suggests that perhaps the contribution of fluorine-19 from the cyclotron is comparable to other sources and further reduced volume may be beneficial.

For both nucleophilic substitution and IEX reactions, small volume synthesis can achieve high SA even from low starting amounts of radioactivity. This is in contrast to macroscale synthesis, where high SA production typically requires starting with Ci levels of radioactivity. Depending on the amount of tracer radioactivity needed, small volume synthesis could therefore reduce the time/cost of cyclotron bombardment, increase safety, and decrease the required amount of shielding required for production.

7.3 Practical Considerations

7.3.1 *Limits of Volume Reduction*

Clearly there are enormous advantages to performing radiochemistry in small volumes. The current EWOD chip geometry can reliably handle volumes as small as ~2 μL , which is limited by the size of the electrodes that are used to load and transport reagent droplets. Scaling down the volume of radiochemical reactions below 2 μL could enable further reductions in precursor cost, further improvements in specific activity (for IEX reactions or biomolecule labeling), further simplification of purification and QC testing, or reduction in the size of the EWOD chip, which leads to cost reduction. Even smaller droplets could be manipulated by scaling down the electrode size and/or reducing the gap between the chip plates. In fact, using specialized fabrication techniques, Nelson and Kim have shown that droplets as small as 100 pL can be manipulated in an EWOD chip [48].

As the volume is scaled down, it is important to be mindful of several issues. First, a certain minimum volume will be needed to solvate the desired amount of the radioisotope complexed with phase transfer catalyst along with the precursor. Another limitation will be the droplet lifetime: at extremely small volume scales, droplets quickly evaporate and may not last sufficiently long to carry out the fluorination reaction. The limit of volume reduction for radiochemistry applications remains to be explored.

7.3.2 Radioisotope Concentration

When considering using small reaction volumes, one must also consider how to produce sufficient quantity (radioactivity) of the tracer for the particular application needed. For preclinical imaging, generally a few mCi is sufficient for a study involving several animals, and with modern scanners, <25–50 μCi is sufficient for a single mouse. On the other hand, imaging of a single patient requires on the order of 10 mCi, while producing a large batch in a radiopharmacy for distribution to imaging centers would require 100s–1000s of mCi. Even higher amounts of the radioisotope are needed at the beginning of the synthesis due to nonideal yields and fluid handling, as well as losses due to decay.

Cyclotrons can readily generate multiple Ci levels of [^{18}F]fluoride in [^{18}O]H₂O to satisfy any of these applications. However, the output volume is typically in the milliliter range, while the capacity of the current EWOD chip (12 mm diameter reaction zone x 150 μm droplet height) is only $\sim 17 \mu\text{L}$, i.e., 1 % of the volume from the cyclotron. From a high-radioactivity bombardment, it would be possible to load as much of tens of mCi of radioisotope into the chip without special measures, but it is not desirable to waste the majority of the radioisotope, and several methods for efficiently concentrating the radioisotope have been developed (Fig. 7.5a).

One approach is to concentrate the [^{18}F]fluoride prior to loading it into the chip via a solid-phase extraction (SPE) process. First, the [^{18}F]fluoride/[^{18}O]H₂O is flowed through a strong anion exchange cartridge (e.g., quaternary methyl ammonium, QMA) to trap the [^{18}F]fluoride. After removing residual water (e.g., with an inert gas flow), an eluent solution (e.g., aqueous K₂CO₃/ K_{2.2.2} or tetrabutylammonium bicarbonate (TBAB), sometimes with MeCN) is passed through the cartridge to release the [^{18}F]fluoride. If the cartridge has sufficiently small bed volume, the volume of eluent solution needed to efficiently collect the [^{18}F]fluoride can be quite low. For example, using commercial cartridges (OPTI-LYNX, Optimize Technologies), Elizarov et al. concentrated 92 % of 876 mCi starting [^{18}F]fluoride into a $\sim 5 \mu\text{L}$ volume [15], our group demonstrated release into $\sim 12 \mu\text{L}$ volume [49], and Lebedev et al. [17] and Bejot et al. [50] demonstrated release into 44 μL volume. This approach can be integrated with microfluidics by using packed-tubing cartridges [15], functionalized porous polymer monoliths [51], packed microchannels [52], or resin-filled inserts [12]. Control of trapping and release processes requires the use of valves with small internal volumes to choose which solution is flowed into the cartridge inlet (i.e., [^{18}F]fluoride or eluent) and whether the cartridge outlet is direct to an [^{18}O]H₂O collection reservoir or the microfluidic chip. Most commonly, this is accomplished with HPLC injection valves, but can also be achieved with on-chip microvalves if they can be conveniently integrated into the device (Fig. 7.5b, c). Once loaded into the chip, the concentrated [^{18}F]fluoride solution is generally evaporated to dryness, and then the subsequent fluorination reaction volume can be controlled by the volume of precursor solution added, provided there is sufficient solvent to dissolve not only the precursor but also the fluoride complex with phase transfer catalyst. Similar trap and release of [^{18}F]fluoride can be accomplished with microfluidic electrochemical flow cells

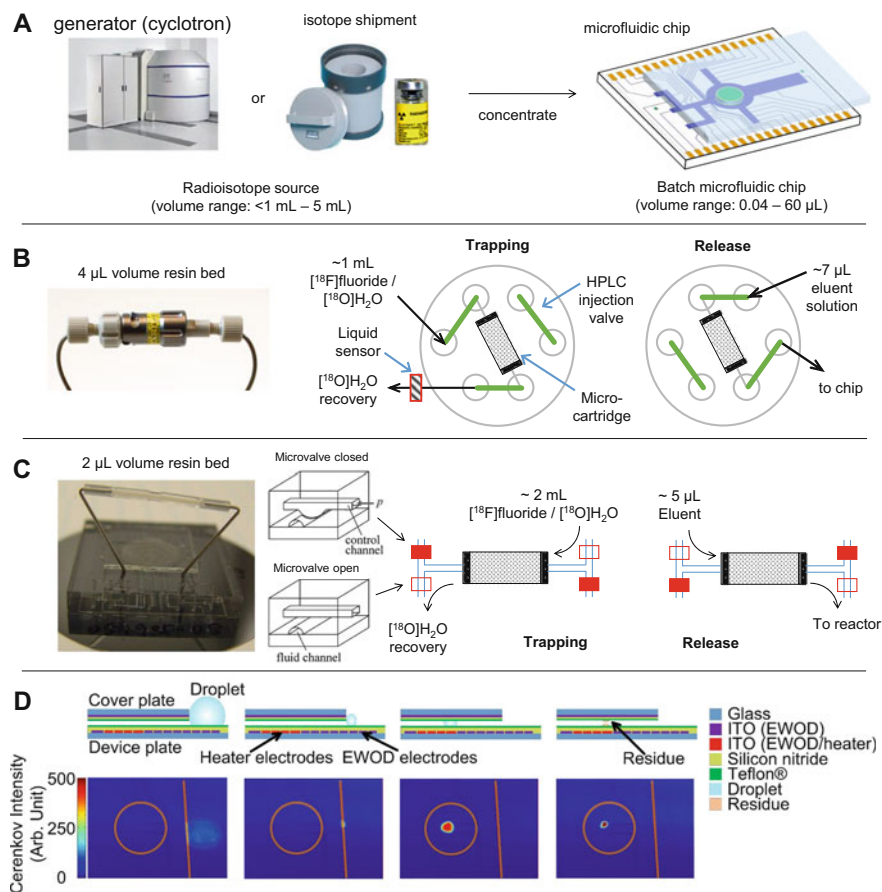


Fig. 7.5 (a) Because the volume of batch microfluidic chips is much smaller than the volume of the radioisotope source, concentration is necessary to ensure sufficient quantity of radioactivity can be loaded onto the chip. (b) Cartridge-based method for concentration described in Ref. [49]. Using an HPLC injection valve with small internal volume, the flow path can be configured in trapping mode, where the $[^{18}\text{F}]$ fluoride/ $[^{18}\text{O}]\text{H}_2\text{O}$ is flowed through a micro-cartridge and the $[^{18}\text{F}]$ fluoride trapped, or a release mode, where a small volume of eluent solution is passed through the cartridge to release the $[^{18}\text{F}]$ fluoride and deliver it onto the chip. (c) Cartridge-based method using on-chip microvalves implemented in a polydimethylsiloxane (PDMS) chip. Pressure applied to “control channels” can open or close nearby “fluid channels” to configure the flow path into trapping and release modes (Adapted from reference [15] © by the Society of Nuclear Medicine and Molecular Imaging, Inc.). (d) Scheme for evaporative concentration of $[^{18}\text{F}]$ fluoride radioisotope. The *top images* show cross-sectional schematics of the concentration process, and the *bottom images* show Cerenkov (radioactivity) images of the *top view* of the chip at corresponding times. *Orange lines and circles* were added to depict the cover plate edge and the reaction site, respectively. Initially, a $200\ \mu\text{L}$ droplet of $[^{18}\text{F}]$ fluoride solution is loaded to the cover plate edge. By activating a nearby heater, the volume of the droplet is reduced to $\sim 5\ \mu\text{L}$ and then pulled into the chip by electrode actuation. (Reproduced from Ref. [25] with permission from the Royal Society of Chemistry.)

[53, 54] where the [^{18}F]fluoride is trapped at an electrode surface by application of positive voltage.

A different approach is to perform the [^{18}F]fluoride concentration directly on chip [25]. A special chip was fabricated where the bottom plate extended beyond the edge of the cover plate to create a platform. A large droplet of [^{18}F]fluoride solution (with phase transfer catalyst) was loaded onto this platform adjacent to the gap between the two EWOD chip plates and then rapidly evaporated down to a small volume that could be transported between the plates (Fig. 7.5d). Because some groups have reported that the anion exchange resin can contribute fluorine-19 contamination [55], this approach may reduce the amount of fluorine-19 in the reaction mixture and thus enable production of PET tracers with higher specific activity. It also has the advantage of not requiring any valves, but the disadvantage of requiring larger chip real estate.

With any of these approaches, it is possible to concentrate a significant fraction of the radioactivity from a cyclotron bombardment into a volume that can be loaded onto the microfluidic chip, enabling radiochemistry to be performed in microliter volumes with high radioactivity.

7.3.3 *Synthesis Automation*

As with radiosynthesis in conventional systems at milliliter volume scales, it is important that the apparatus is operated in an automated fashion within radiation shielding to ensure the safety of the operator preparing the PET tracer. Fully automated synthesizers have been developed based on some of the earlier reports of batch microfluidic chips, complete with reagent delivery, radioisotope concentration, synthesis, and cartridge-based purification or interfacing with an HPLC system [15, 17, 50, 56].

For the more recent EWOD microfluidic platform, many aspects of automating the overall system have been demonstrated. Two approaches have been developed for loading reagents from off-chip reservoirs (e.g., standard septum-capped glass reagent vials) into the chip. One simple approach uses an electronically controlled syringe pump to precisely dispense the desired volume of reagent after compensating for evaporation losses at the dispensing tip [57]. Another approach was developed in collaboration with Sofie Biosciences, Inc. to avoid the use of complex, difficult-to-clean components such as syringe pumps and valves, instead of relying on simple disposable fluidic elements such as needles and tubing. Inert gas pressure and gravitational force were used to apply forward and reverse driving forces, respectively, to deliver repeatable volumes to the chip [58]. A multi-reagent loading interface was developed based on this principle and was integrated with a simple cartridge-based method for upstream [^{18}F]fluoride concentration and an automated method for downstream collection of the crude product from the chip and interfacing with miniature solid-phase extraction cartridges or analytical-scale HPLC for purification [34]. Some preliminary progress to develop methods for on-chip purification has also been made including removal of unreacted [^{18}F]fluoride

using an alumina surface [35] or beads [36], and more complete separation may be possible by performing on-chip solid-phase extraction. A prototype of a complete EWOD-based PET tracer production system suitable for benchtop operation is under development at Sofie Biosciences in collaboration with our group.

7.4 Conclusions and Outlook

The development of batch microfluidic devices may provide an ideal platform to harness the numerous advantages of performing the synthesis of PET radiotracers in small volumes, including reduced reagent consumption, improved specific activity, reduced radiolysis, and synthesizer miniaturization. In particular, the EWOD platform is compatible with diverse reaction conditions and provides a convenient means to digitally manipulate droplets to perform diverse multistep reactions. By combining these devices with technologies for concentration of radioisotopes into an automated platform, it will become possible to produce not only batches on demand for research use but even large-scale batches in a radiopharmacy for distribution purposes. This microvolume radiochemistry technique could also be a particularly good match for isotopic exchange and biomolecule labeling reactions and could enable novel chemistries by boosting [^{18}F]fluoride concentration by orders of magnitude. As a tool for remotely and safely handling small volumes, the EWOD microfluidic platform could open up opportunities for researchers to uncover additional benefits of radiochemistry in extremely small volumes.

Acknowledgments The authors gratefully acknowledge support for writing this review from the National Institute of Biomedical Imaging and Bioengineering (grant R21EB015540), the National Institute on Aging (grant R21AG049918), as well as Sofie Biosciences, Inc., and the National Institute of Mental Health (grant R44MH097271).

Open Access This chapter is distributed under the terms of the Creative Commons Attribution-Noncommercial 2.5 License (<http://creativecommons.org/licenses/by-nc/2.5/>) which permits any noncommercial use, distribution, and reproduction in any medium, provided the original author(s) and source are credited.

The images or other third party material in this chapter are included in the work's Creative Commons license, unless indicated otherwise in the credit line; if such material is not included in the work's Creative Commons license and the respective action is not permitted by statutory regulation, users will need to obtain permission from the license holder to duplicate, adapt or reproduce the material.

References

1. Phelps ME. Positron emission tomography provides molecular imaging of biological processes. *PNAS*. 2000;97:9226–33.
2. Kelloff GJ, Hoffman JM, Johnson B, et al. Progress and promise of FDG-PET imaging for cancer patient management and oncologic drug development. *Clin Cancer Res*. 2005;11:2785–808.

3. Lasne M-C, Perrio C, Rouden J, Barré L, Roeda D, Dolle F, Crouzel C. Chemistry of β^+ -emitting compounds based on fluorine-18. In: Krause W, editor. *Contrast agents II*. Berlin/Heidelberg: Springer; 2002. p. 201–58.
4. Keng PY, Esterby M, van Dam RM. Emerging technologies for decentralized production of PET tracers. In: Hsieh C-H, editor. *Positron emission tomography – current clinical and research aspects*. InTech; 2012. p. 153–82.
5. Rensch C, Jackson A, Lindner S, Salvamoser R, Samper V, Riese S, Bartenstein P, Wängler C, Wängler B. Microfluidics: a groundbreaking technology for PET tracer production? *Molecules*. 2013;18:7930–56.
6. Miller PW, deMello AJ, Gee AD. Application of microfluidics to the ultra-rapid preparation of fluorine-18 labelled compounds. *Curr Radiopharm*. 2010;3:254–62.
7. Watts P, Pascali G, Salvadori PA. Positron emission tomography radiosynthesis in microreactors. *J Flow Chem*. 2012;2:37–42.
8. McMullen JP, Jensen KF. Integrated microreactors for reaction automation: new approaches to reaction development. *Annu Rev Anal Chem*. 2010;3:19–42.
9. Gillies JM, Prenant C, Chimon GN, Smethurst GJ, Perrie W, Hamblett I, Dekker B, Zweit J. Microfluidic reactor for the radiosynthesis of PET radiotracers. *Appl Radiat Isot*. 2006;64:325–32.
10. Steel CJ, O'Brien AT, Luthra SK, Brady F. Automated PET radiosyntheses using microfluidic devices. *J Label Compd Radiopharm*. 2007;50:308–11.
11. Wester H-J, Schoultz BW, Hultsch C, Henriksen G. Fast and repetitive in-capillary production of [^{18}F]FDG. *Eur J Nucl Med Mol Imaging*. 2009;36:653–8.
12. Pascali G, Watts P, Salvadori PA. Microfluidics in radiopharmaceutical chemistry. *Nucl Med Biol*. 2013;40:776–87.
13. Rensch C, Lindner S, Salvamoser R, et al. A solvent resistant lab-on-chip platform for radiochemistry applications. *Lab Chip*. 2014;14:2556–64.
14. Arima V, Pascali G, Lade O, et al. Radiochemistry on chip: towards dose-on-demand synthesis of PET radiopharmaceuticals. *Lab Chip*. 2013;13(12):2328–36.
15. Lee C-C, Sui G, Elizarov A, et al. Multistep synthesis of a radiolabeled imaging probe using integrated microfluidics. *Science*. 2005;310:1793–6.
16. Elizarov AM, van Dam RM, Shin YS, Kolb HC, Padgett HC, Stout D, Shu J, Huang J, Daridon A, Heath JR. Design and optimization of coin-shaped microreactor chips for PET radiopharmaceutical synthesis. *J Nucl Med*. 2010;51:282–7.
17. Tseng W-Y, Cho JS, Ma X, Kunihiro A, Chatziioannou A, van Dam RM. Toward reliable synthesis of radiotracers for positron emission tomography in PDMS microfluidic chips: study and optimization of the [^{18}F] fluoride drying process. In: *Technical proceedings of the 2010 NSTI nanotechnology conference and trade show, Anaheim, CA*. Boca Raton: CRC Press; 2010. p. 472–5.
18. Lebedev A, Miraghaie R, Kotta K, Ball CE, Zhang J, Buchsbaum MS, Kolb HC, Elizarov A. Batch-reactor microfluidic device: first human use of a microfluidically produced PET radiotracer. *Lab Chip*. 2012;13:136–45.
19. Liu K, Lepin EJ, Wang M-W, et al. Microfluidic-based ^{18}F -labeling of biomolecules for immuno-positron emission tomography. *Mol Imaging*. 2011;10:168–76.
20. Zeng D, Desai AV, Ranganathan D, Wheeler TD, Kenis PJA, Reichert DE. Microfluidic radiolabeling of biomolecules with PET radiometals. *Nucl Med Biol*. 2013;40:42–51.
21. Keng PY, Chen S, Ding H, et al. Micro-chemical synthesis of molecular probes on an electronic microfluidic device. *PNAS*. 2012;109:690–5.
22. Reichert DE. A digital revolution in radiosynthesis. *J Nucl Med*. 2014;55:181–2.
23. Sadeghi S, Ding H, Shah GJ, Chen S, Keng PY, Kim C-J “CJ”, van Dam RM. On chip droplet characterization: a practical, high-sensitivity measurement of droplet impedance in digital microfluidics. *Anal Chem*. 2012;84:1915–23.
24. Javed MR, Chen S, Kim H-K, Wei L, Czernin J, Kim C-J “CJ”, Dam RM van, Keng PY. Efficient radiosynthesis of 3'-deoxy-3'- ^{18}F -fluorothymidine using electrowetting-on-dielectric digital microfluidic chip. *J Nucl Med*. 2014;55:321–8.

25. Javed MR, Chen S, Lei J, Collins J, Sergeev M, Kim H-K, Kim C-J, van Dam RM, Keng PY. High yield and high specific activity synthesis of [¹⁸F]fallypride in a batch microfluidic reactor for micro-PET imaging. *Chem Commun.* 2014;50:1192–4.
26. Chen S, Javed MR, Kim H-K, Lei J, Lazari M, Shah GJ, van Dam M, Keng PY, Kim C-J. Radiolabelling diverse positron emission tomography (PET) tracers using a single digital microfluidic reactor chip. *Lab Chip.* 2014;14:902–10.
27. Koag MC, Kim H-K, Kim AS. Efficient microscale synthesis of [¹⁸F]-2-fluoro-2-deoxy-d-glucose. *Chem Eng J.* 2014;258:62–8.
28. Koag MC, Kim H-K, Kim AS. Fast and efficient microscale radiosynthesis of 3'-deoxy-3'-[¹⁸F]fluorothymidine. *J Fluor Chem.* 2014;166:104–9.
29. Fawdry RM. Radiolysis of 2-[¹⁸F]fluoro-2-deoxy-d-glucose (FDG) and the role of reductant stabilisers. *Appl Radiat Isot.* 2007;65:1193–201.
30. Búriová E, Macáček F, Melichar F, Kropáček M, Procházka L. Autoradiolysis of the 2-deoxy-2-[¹⁸F]fluoro-D-glucose radiopharmaceutical. *J Radioanal Nucl Chem.* 2005;264:595–602.
31. Jacobson MS, Dankwart HR, Mahoney DW. Radiolysis of 2-[¹⁸F]fluoro-2-deoxy-d-glucose ([¹⁸F]FDG) and the role of ethanol and radioactive concentration. *Appl Radiat Isot.* 2009;67:990–5.
32. Levin CS, Hoffman EJ. Calculation of positron range and its effect on the fundamental limit of positron emission tomography system spatial resolution. *Phys Med Biol.* 1999;44:781.
33. Rensch C, Waengler B, Yaroshenko A, Samper V, Baller M, Heumesser N, Ulin J, Riese S, Reischl G. Microfluidic reactor geometries for radiolysis reduction in radiopharmaceuticals. *Appl Radiat Isot.* 2012;70:1691–7.
34. Lazari M, Collins J, Shen B, Farhoud M, Yeh D, Maraglia B, Chin FT, Nathanson DA, Moore M, van Dam RM. Fully automated production of diverse ¹⁸F-labeled PET tracers on the ELIXYS multireactor radiosynthesizer without hardware modification. *J Nucl Med Technol.* 2014;42:203–10.
35. Shah GJ, Lei J, Chen S, Kim C-J “CJ,” Keng PY, Van Dam RM. Automated injection from EWOD digital microfluidic chip into HPLC purification system. In: *Proceedings of the 16th international conference on miniaturized systems for chemistry and life sciences, Okinawa.* London: Royal Society of Chemistry; 2012. p. 356–8.
36. Chen S, Lei J, van Dam RM, Keng P-Y, Kim C-J “CJ”. Planar alumina purification of ¹⁸F-labeled radiotracer synthesis on EWOD chip for positron emission tomography (PET). In: *Proceedings of the 16th international conference on miniaturized systems for chemistry and life sciences, Okinawa.* London: Royal Society of Chemistry; 2012. p. 1771–3.
37. Chen S, Dooraghi A, Lazari M, van Dam RM, Chatziioannou A, Kim C-J. On-chip product purification for complete microfluidic radiotracer synthesis. In: *Proceedings of the 27th IEEE international conference on micro electro mechanical systems (MEMS), San Francisco, CA.* Piscataway: IEEE; 2014. p. 284–7.
38. Tarn MD, Pascali G, De Leonardi F, Watts P, Salvadori PA, Pamme N. Purification of 2-[¹⁸F]fluoro-2-deoxy-d-glucose by on-chip solid-phase extraction. *J Chromatogr A.* 2013;1280:117–21.
39. Hume SP, Gunn RN, Jones T. Pharmacological constraints associated with positron emission tomographic scanning of small laboratory animals. *Eur J Nucl Med Mol Imaging.* 1998;25:173–6.
40. Lapi SE, Welch MJ. A historical perspective on the specific activity of radiopharmaceuticals: What have we learned in the 35 years of the ISRC? *Nucl Med Biol.* 2013;40:314–20.
41. Satyamurthy N, Amarasekera B, Alvord CW, Barrio JR, Phelps ME. Tantalum [¹⁸O]water target for the production of [¹⁸F]fluoride with high reactivity for the preparation of 2-deoxy-2-[¹⁸F]fluoro-D-glucose. *Mol Imaging Biol.* 2002;4:65–70.
42. Solin O, Bergman J, Haaparanta M, Reissell A. Production of ¹⁸F from water targets. Specific radioactivity and anionic contaminants. *Int J Radiat Applications and Instrumentation Part A Applied Radiation and Isotopes.* 1988;39:1065–71.

43. Füchtner F, Preusche S, Mäding P, Zessin J, Steinbach J. Factors affecting the specific activity of [^{18}F]fluoride from a [^{18}O]water target. *Nuklearmedizin*. 2008;47:116–9.
44. Berridge MS, Apana SM, Hersh JM. Teflon radiolysis as the major source of carrier in fluorine-18. *J Label Compd Radiopharm*. 2009;52:543–8.
45. Lazari M, Sergeev M, Liu Z, Perrin DM, van Dam RM. Study of specific activity in isotopic exchange radiofluorination performed on a microfluidic device. Seoul: World Molecular Imaging Congress; 2014.
46. Sergeev M, Lazari M, Collins J, Morgia F, Javed MR, Keng PY, van Dam RM. Investigation of effect of reaction volume on specific activity in macro- and microscale fluorine-18 radiosynthesis. In: Proceedings of the 6th international symposium on microchemistry and microsystems (ISMM), Singapore; 2014. p. 77–8.
47. Ting R, Lo J, Adam MJ, Ruth TJ, Perrin DM. Capturing aqueous [^{18}F]fluoride with an arylboronic ester for PET: synthesis and aqueous stability of a fluorescent [^{18}F]labeled aryltrifluoroborate. *J Fluor Chem*. 2008;129:349–58.
48. Liu Z, Li Y, Lozada J, Pan J, Lin K-S, Schaffer P, Perrin DM. Rapid, one-step, high yielding ^{18}F -labeling of an aryltrifluoroborate bioconjugate by isotope exchange at very high specific activity. *J Label Compd Radiopharm*. 2012;55:491–6.
49. Nelson WC, Kim JY. Monolithic fabrication of EWOD chips for picoliter droplets. *J Microelectromech Syst*. 2011;20:1419–27.
50. Lazari M, Narayanam MK, Murphy JM, Van Dam MR. Automated concentration of ^{18}F -fluoride into microliter volumes. In: 21st international symposium on radiopharmaceutical sciences, Columbia, MO; 2015.
51. Bejot R, Elizarov AM, Ball E, Zhang J, Miraghaie R, Kolb HC, Gouverneur V. Batch-mode microfluidic radiosynthesis of N-succinimidyl-4- ^{18}F fluorobenzoate for protein labelling. *J Label Compd Radiopharm*. 2011;54:117–22.
52. Ismail R, Irribarren J, Javed MR, Machness A, van Dam M, Keng PY. Cationic imidazolium polymer monoliths for efficient solvent exchange, activation and fluorination on a continuous flow system. *RSC Adv*. 2014;4:25348–56.
53. De Leonardi F, Pascali G, Salvadori PA, Watts P, Pamme N. On-chip pre-concentration and complexation of [^{18}F]fluoride ions via regenerable anion exchange particles for radiochemical synthesis of positron emission tomography tracers. *J Chromatogr A*. 2011;1218:4714–9.
54. Sadeghi S, Liang V, Cheung S, Woo S, Wu C, Ly J, Deng Y, Eddings M, van Dam RM. Reusable electrochemical cell for rapid separation of [^{18}F]fluoride from [^{18}O]water for flow-through synthesis of ^{18}F -labeled tracers. *Appl Radiat Isot*. 2013;75:85–94.
55. Saiki H, Iwata R, Nakanishi H, Wong R, Ishikawa Y, Furumoto S, Yamahara R, Sakamoto K, Ozeki E. Electrochemical concentration of no-carrier-added [^{18}F]fluoride from [^{18}O]water in a disposable microfluidic cell for radiosynthesis of ^{18}F -labeled radiopharmaceuticals. *Appl Radiat Isot*. 2010;68:1703–8.
56. Lu S, Giamis AM, Pike VW. Synthesis of [^{18}F]fallypride in a micro-reactor: rapid optimization and multiple-production in small doses for micro-PET studies. *Curr Radiopharm*. 2009;2:1–13.
57. Van Dam RM, Elizarov AM, Ball CE, et al. Automated microfluidic-chip-based stand-alone instrument for the synthesis of radiopharmaceuticals on human-dose scales. In: Technical proceedings of the 2007 NSTI nanotechnology conference and trade show, Santa Clara, CA. Boca Raton: CRC Press; 2007. p. 300–3.
58. Ding H, Sadeghi S, Shah GJ, Chen S, Keng PY, Kim CJ, van Dam M. Accurate dispensing of volatile reagents on demand for chemical reactions in EWOD chips. *Lab Chip*. 2012;12:3331–40.
59. Shah GJ, Ding H, Sadeghi S, Chen S, Kim C-J, van Dam RM. Milliliter-to-microliter platform for on-demand loading of aqueous and non-aqueous droplets to digital microfluidics. In: Proceedings of the 16th international solid-state sensors, actuators and microsystems conference (TRANSDUCERS), Beijing. Piscataway: IEEE; 2011. p. 1260–3.

60. Chen Y-C, Liu K, Shen CK-F, van Dam RM. On-demand generation and mixing of liquid-in-gas slugs with digitally programmable composition and size. *J Micromech Microeng.* 2015;25:084006.
61. Wheeler AR, Moon H, Kim C-J, Loo JA, Garrell RL. Electrowetting-based microfluidics for analysis of peptides and proteins by matrix-assisted laser desorption/ionization mass spectrometry. *Anal Chem.* 2004;76:4833–8.
62. Cho SK, Moon H, Kim C-J. Creating, transporting, cutting, and merging liquid droplets by electrowetting-based actuation for digital microfluidic circuits. *J MEMS.* 2003;12:70–80.
63. Barbulovic-Nad I, Yang H, Park P, Wheeler A. Digital microfluidics for cell-based assays. *Lab Chip.* 2008;8:519.